Numerical Solution for the Falkner-Skan Boundary Layer Viscous Flow over a Wedge

[1] Mohammad Mehdi Keshtkar, [2] Mohammad Ezatabadi

[1] Assistant Professor of Mechanical Engineering, Islamic Azad University, Kerman Branch, Iran
[2] MS.c student of Mechanical Engineering, Islamic Azad University, Kerman Branch, Iran

ABSTRACT : *We explore the problem of the Falkner-Skan boundary layer flow past a wedge considering the velocity slip condition and nanofluid. The governing partial differential equation is transformed into an ordinary differential equation. The numerical results of the resulting ordinary system are obtained using Matlab software. The effect of the slip parameter on the flow and the presence of the nanofluids are discussed.*

KEYWORDS : *Boundary layer, Blasius flow, Falkner-Skan flow, Similarity Solution, nanofluid.*

I. INTRODUCTION

The boundary layer theory distinctly elucidates the steady-state flow in excess of a flat plate at zero occurrence angle which is recognized as Blasius flow. The Falkner–Skan equation was offered by Falkner and Skan. As its name offers, The Falkner–Skan equation was presented by Falkner and Skan. Falkner and Skan(1931) developed a study about viscous fluid submerged the flow in excess of a static wedge. They expanded a similarity transformation that can be utilized to reduce the limited differential boundary layer equations to a nonlinear third-order normal differential equation and after that explained it arithmetically. A large amount of literature on this subject has been referred to in the books by different researchers. It is well known that conventional heat transfer fluids such as water, mineral oil and ethylene glycol have, in general, poor heat transfer properties compared to those of most solids. An innovative way of improving the heat transfer of fluids is to suspend small solid particles in the fluids. This *new* kind of fluids named as "nanofluids" was introduced in 1995 by Choi[1]. The term nanofluid is used to describe a solid liquid mixture which consists of base liquid with low volume fraction of high conductivity solid nanoparticles. These fluids enhance enormously the thermal conductivity of the base fluid which is beyond the explanation of any existing theory.

They are also very stable and have no additional problems, such as sedimentation, erosion, additional pressure drop and non-Newtonian behavior, due to the tiny size of nanoelements and the low volume fraction of nanoelements required for conductivity enhancement. The use of particles of nanometer dimension was first continuously studied by a research group at the Argonne National Laboratory around a decade ago. These suspended nanoparticles can change the transport and thermal properties of the base fluid. B.D. Ganapol[2] presented a new highly accurate algorithm for the solution of the Falkner-Skan equation of boundary layer theory. The algorithm, based on a Maclaurin series representation. Norihan Md. Arifin, Roslinda Nazar & Ioan Pop[3] studied the classical problems of forced convection boundary layer flow and heat transfer near the stagnation point on a permeable stretching/shrinking surface in a nanofluid theoretically. It was found that the nanoparticle volume fraction substantially affects the fluid flow and heat transfer characteristics.Norfifah Bachok,

Anuar Ishak & Ioan Pop[4] performed an analysis the heat transfer characteristics of steady two-dimensional boundary layer flow past a moving permeable flat plate in a nanofluid. The effects of uniform suction and injection on the flow field and heat transfer characteristics are numerically studied by using an implicit finite difference method. It is found that dual solutions exist when the plate and the free stream move in the opposite directions. The results indicate that suction delays the boundary layer separation, while injection accelerates it. Nor Azizah Yacob, Anuar Ishak, Ioan Pop and Kuppalapalle Vajravelu[5] survey the problem of a steady boundary layer shear flow over a stretching/shrinking sheet in a nanofluid. The effects of nanoparticle volume fraction, the type of nanoparticles, the convective parameter, and the thermal conductivity on the heat transfer characteristics are discussed. It is found that the heat transfer rate at the surface increases with increasing nanoparticle volume fraction while it decreases with the convective parameter. Moreover, the heat transfer rate at the surface of Cu-water nanofluid is higher than that at the surface of Ag-water nanofluid even though the thermal conductivity of Ag is higher than that of Cu. Meraj Mustafa, Muhammad A. Farooq,

Tasawar Haya, Ahmed Alsaedi[6] investigated the stagnation-point flow of nanofluid past an exponentially stretching sheet. The presence of Brownian motion and thermophoretic effects yields a coupled nonlinear boundary-value problem (BVP).Local similarity solutions are obtained by homotopy analysis method (HAM), which enables them to investigate the effects of parameters at a fixed location above the sheet. The results indicate that temperature and the thermal boundary layer thickness appreciably increase when the Brownian motion and thermophoresis effects are strengthened. Moreover the nanoparticles volume fraction is found to increase when the thermophoretic effect intensifies. Muatazz Abdolhadi Bashir, Mustafa Mamat and Ilyani Abdullah[7] explored the problem of the Falkner-Skan boundary layer flow past a wedge considering the velocity slip condition. The numerical results of the resulting ordinary system were obtained using an implicit finite difference under Matlab software. The effect of the slip parameter on the flow was discussed.

II. PROBLEM FORMULATION

Flow over the top of a wedge can be modeled as an external flow $U(x)$ with a pressure gradient given by the inviscid flow solution. The angle of the wedge is given as $\beta\pi$.(Figure 1)
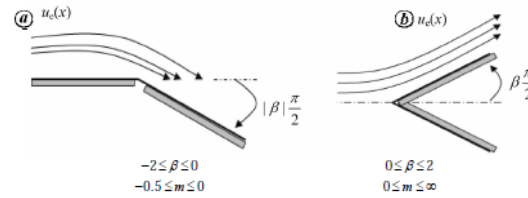

Fig.1 Different potential flows over a wedge. a. flow around a corner(diffusion).b. wedge flow

The external flow velocity and pressure gradients are given by:

$$U(x) = bx^m \tag{1}$$

$$\frac{\partial P}{\partial x} = -\rho U(x)\frac{dU(x)}{dx} = -m\rho b^2 x^{-2m-1} \tag{2}$$

Where U is the external velocity, P is the pressure, ρ is the density, and x is the position along the wedge. The coefficient b is a function of the flow geometry. As long as the boundary layer is relatively thin, the external flow, and the pressure gradient will be independent of the thickness of the boundary layer.
The exponent m is a function of the angle β:

$$m = \frac{\beta}{2-\beta} \tag{3}$$

The flow near the wedge will be governed by the boundary-layer equations. The equation for continuity is identical to the flat-plate case:

$$\frac{\partial u}{\partial x}+\frac{\partial v}{\partial y} = 0 \tag{4}$$

For steady flow in a boundary layer, the x-momentum equation is given by:

$$u\frac{\partial u}{\partial x} + v\frac{\partial u}{\partial y} = -\frac{1}{\rho}\frac{dP(x)}{dx} + v\frac{\partial^2 u}{\partial y^2} \tag{5}$$

where u is the x velocity, v is the y velocity, and v is the kinematic viscosity. These equations can then be transformed, using the nondimensionalizations and nondimensional stream functions developed by Falkner and Skan. These nondimensionalizations are similar to, but not identical to, those used by Blasius. A nondimensional flow coordinate η is formed by combining x and y with the other flow variables:

$$\eta = y\sqrt{\frac{m+1}{2}\frac{b}{v}}\ x^{\frac{m-1}{2}} \tag{6}$$

A nondimensional stream function $f(\eta)$ is found from the dimensional stream function ψ:

$$\psi(x, y) = \sqrt{\frac{2bv}{m+1}} \; x^{\frac{m+1}{2}} f(\eta) \tag{7}$$

The nondimensional velocities are given as:

$$u^* = \frac{u}{U(x)} = f'(\eta) \tag{8}$$

$$v^* = \frac{v}{\sqrt{\frac{2}{m+1}vbx^{m-1}}} = \left[f(\eta) - \frac{m-1}{m+1}\eta f'(\eta)\right] \tag{9}$$

A governing equation for f can be found by substituting these nondimensional terms into the *x*-momentum equation:

$$f'''(\eta) + \beta_0 f(\eta) f''(\eta) + \beta(1 - f'(\eta)^2) \\ = 0 \qquad \eta \epsilon [0, \infty) \tag{10}$$

For the no-slip case, the boundary conditions are:

$$u^*(y = 0) = 0 \;\; \rightarrow f'(\eta = 0) = 0 \tag{11}$$

$$v^*(y = 0) = 0 \;\; \rightarrow f(\eta = 0) = 0 \tag{12}$$

$$u^*(y \rightarrow \infty) = 1 \;\; \rightarrow f'(\eta \rightarrow \infty) = 1 \tag{13}$$

III. RESULTS AND DISCUSION

B.D. Ganapol[2] submitted variation of velocity profile with α namely f'(0) (shooting angle)for Homann flow in Figure 2.
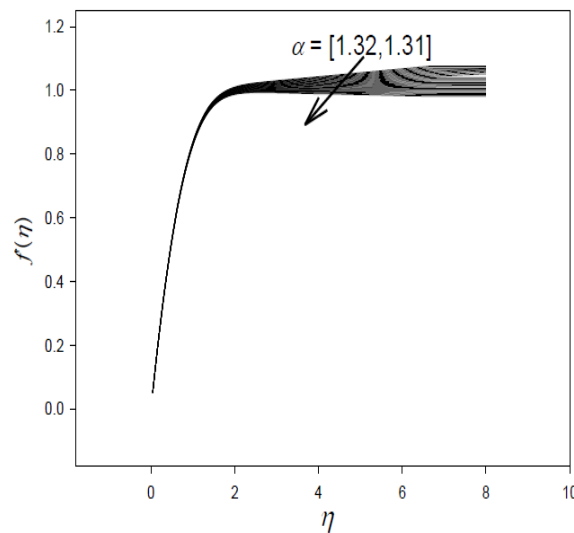

Fig.2 Variation of velocity profile with α for Homann flow

We at first find the shooting angle, namely f''(0) for transform the BVP problem to IVP problem and next solve this IVP with a code in Matlab software and then draw above chart as Figure 3.
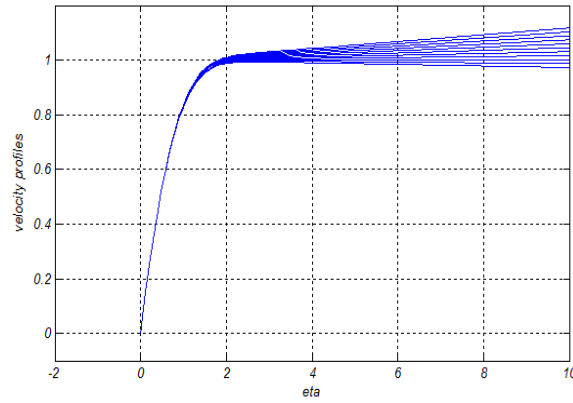
20

Fig.3 Variation of velocity profile with f''(0)(shooting angle) for Homann flow

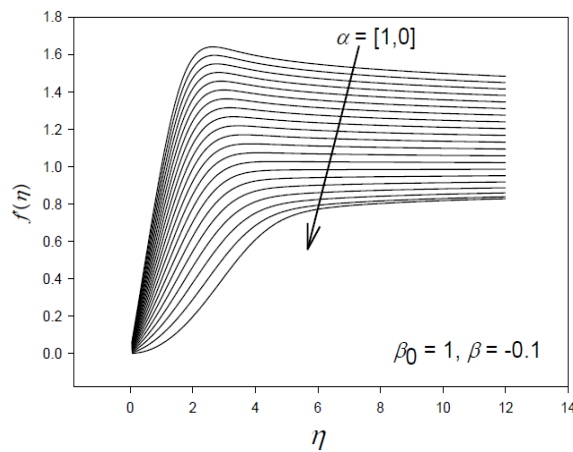Also B.D. Ganapol[2] submitted variation of the velocity profile for β = -0.1 according to Figure4.

Fig.4 Variation of the velocity profile for β=-0.1

The true value for α is the value that velocity profile approach to number 1(third boundary condition) but in this chart, velocity profiles are draw for 20 amount of α from 0 to 1. We draw this chart with Matlab software as Figure 5.
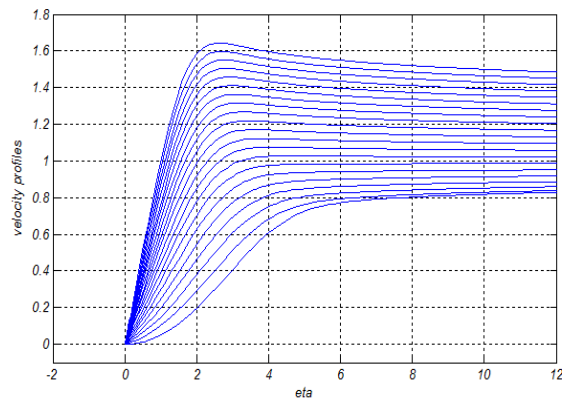

Fig.5 Variation of the velocity profile for 0≤ α≤1 and β=-0.1

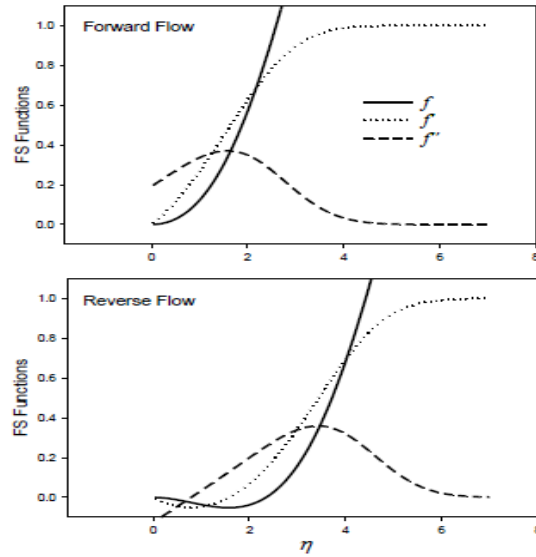In Fig 6. for β=-0.16, the F-S functions are contrasted for forward and reversed flow.

Fig.6 Forward & reverse flow for β=-0.16

We draw one set of these charts with Matlab software in Figure7. In this figure, the variation of f(η), f'(η) and f''(η) with η are compared.
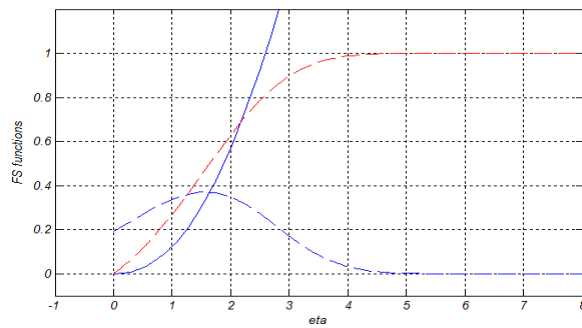
Fig.7 F-S functions variation

B.D. Ganapol [2] submitted the Blasius flow profiles as Table 1.

Table 1 Blasius flow profiles

η	f	f'	f''
0.0E+00	0.000000000E+00	0.000000000E+00	3.320573362E-01
2.0E-01	6.640999715E-03	6.640779210E-02	3.319838371E-01
4.0E-01	2.655988402E-02	1.327641608E-01	3.314698442E-01
6.0E-01	5.973463750E-02	1.989372524E-01	3.300791276E-01
8.0E-01	1.061082208E-01	2.647091387E-01	3.273892701E-01
1.0E+00	1.655717258E-01	3.297800312E-01	3.230071167E-01
1.2E+00	2.379487173E-01	3.937761044E-01	3.165891911E-01
1.4E+00	3.229815738E-01	4.562617647E-01	3.078653918E-

			01
1.6E+00	4.203207655E-01	5.167567844E-01	2.966634615E-01
1.8E+00	5.295180377E-01	5.747581439E-01	2.829310173E-01
2.0E+00	6.500243699E-01	6.297657365E-01	2.667515457E-01
2.2E+00	7.811933370E-01	6.813103772E-01	2.483509132E-01
2.4E+00	9.222901256E-01	7.289819351E-01	2.280917607E-01
2.6E+00	1.072505977E+00	7.724550211E-01	2.064546268E-01
2.8E+00	1.230977302E+00	8.115096232E-01	1.840065939E-01
3.0E+00	1.396808231E+00	8.460444437E-01	1.613603195E-01
3.2E+00	1.569094960E+00	8.760814552E-01	1.391280556E-01
3.4E+00	1.746950094E+00	9.017612214E-01	1.178762461E-01
3.6E+00	1.929525170E+00	9.233296659E-01	9.808627878E-02
3.8E+00	2.116029817E+00	9.411179967E-01	8.012591814E-02
4.0E+00	2.305746418E+00	9.555182298E-01	6.423412109E-02
4.2E+00	2.498039663E+00	9.669570738E-01	5.051974749E-02
4.4E+00	2.692360938E+00	9.758708321E-01	3.897261085E-02
4.6E+00	2.888247990E+00	9.826835008E-01	2.948377201E-02
4.8E+00	3.085320655E+00	9.877895262E-01	2.187118635E-02
5.0E+00	3.283273665E+00	9.915419002E-01	1.590679869E-02
5.2E+00	3.481867612E+00	9.942455354E-01	1.134178897E-02
5.4E+00	3.680919063E+00	9.961553040E-01	7.927659815E-03
5.6E+00	3.880290678E+00	9.974777682E-01	5.431957680E-03
5.8E+00	4.079881939E+00	9.983754937E-01	3.648413667E-03
6.0E+00	4.279620923E+00	9.989728724E-01	2.402039844E-03
6.2E+00	4.479457297E+00	9.993625417E-01	1.550170691E-03
6.4E+00	4.679356615E+00	9.996117017E-01	9.806151170E-04
6.6E+00	4.879295811E+00	9.997678702E-01	6.080442648E-04
6.8E+00	5.079259772E+00	9.998638190E-01	3.695625701E-04
7.0E+00	5.279238811E+00	9.999216041E-01	2.201689553E-04
7.2E+00	5.479226847E+00	9.999557173E-01	1.285698072E-

			04
7.4E+00	5.679220147E+00	9.999754577E-01	7.359298339E-05
7.6E+00	5.879216466E+00	9.999866551E-01	4.129031111E-05
7.8E+00	6.079214481E+00	9.999928812E-01	2.270775140E-05
8.0E+00	6.279213431E+00	9.999962745E-01	1.224092624E-05
8.2E+00	6.479212887E+00	9.999980875E-01	6.467978611E-06
8.4E+00	6.679212609E+00	9.999990369E-01	3.349939753E-06
8.6E+00	6.879212471E+00	9.999995242E-01	1.700667989E-06
8.8E+00	7.079212403E+00	9.999997695E-01	8.462841214E-07

We obtain this table with Matlab software as Table 2 .In this table the variation of f(η), f'(η) and f''(η) with η from η=0 to η=8.8 are submitted. Our result are complied with the Ganapol's result with a good precision.

Table 2 Blasius Flow Profiles

η	f	f '	f "

0.000000	0.000000	0.000000	0.332000
0.283571	0.013347	0.094131	0.331791
0.472719	0.037084	0.156828	0.331031
0.665422	0.073437	0.220473	0.329306
0.858125	0.122017	0.283661	0.326250
1.050829	0.182716	0.346103	0.321526
1.243532	0.255347	0.407451	0.314844
1.463532	0.352518	0.475646	0.304530
1.683532	0.464419	0.541232	0.291185
1.903532	0.590418	0.603538	0.274811
2.123532	0.729710	0.661930	0.255601
2.343532	0.881347	0.715826	0.233943
2.563532	1.044297	0.764740	0.210456
2.783532	1.217437	0.808343	0.185866
3.003532	1.399577	0.846489	0.160963
3.223532	1.589498	0.879205	0.136558
3.443532	1.786032	0.906682	0.113422
3.663532	1.988074	0.929256	0.092178
3.883532	2.194590	0.947396	0.073248
4.047232	2.350599	0.958356	0.060806
4.210933	2.508243	0.967398	0.049833
4.374633	2.667233	0.974753	0.040330
4.668379	2.955094	0.984490	0.026695
4.798424	3.083333	0.987647	0.021932
5.058515	3.340864	0.992318	0.014452
5.188561	3.470023	0.994008	0.011576
5.448652	3.728894	0.996419	0.007250
5.690917	3.970475	0.997825	0.004551
5.803137	4.082477	0.998283	0.003629
6.027575	4.306609	0.998932	0.002270
6.223454	4.502316	0.999294	0.001474
6.419332	4.698081	0.999527	0.000940
6.684704	4.963355	0.999711	0.000495

6.855666	5.134274	0.999780	0.000322
7.020676	5.299252	0.999823	0.000209
7.285944	5.564478	0.999863	0.000102
7.468706	5.747217	0.999878	0.000061
7.669654	5.948141	0.999887	0.000034
7.870602	6.149067	0.999892	0.000018
8.097762	6.376203	0.999895	0.000009
8.211342	6.489771	0.999896	0.000006
8.443691	6.722096	0.999897	0.000003
8.681230	6.959611	0.999897	0.000001
8.800000	7.078368	0.999897	0.000001

Norihan Md. Arifin, Roslinda Nazar & Ioan Pop[3] studied viscous flow due to a permeable stretching/shrinking sheet in a nanofluid.

Table 3 Thermophysical properties of fluid and nanoparticles

Physical properties	Fluid phase(water)
Cu Ag	
C_p(J/kg K)	4179
385 235	
ρ(kg/m^3)	997.1
8933 10500	
k(W/mK)	0.613
400 429	

The governing equation is:

$$\frac{1}{(1-\phi)^{2.5}\left(1-\phi+\frac{\phi\rho_s}{\rho_f}\right)}f''' + mff'' + 1 - f'^2 = 0 \tag{14}$$

$$f(0)=s, \ f'(0)=\lambda, \ f'(\eta \rightarrow \infty) \rightarrow 1 \tag{15}$$

Here s is the suction ($s>0$) parameter, $\lambda = c/a$ is the stretching ($\lambda > 0$) or shrinking ($\lambda < 0$) parameter and φ is the nanoparticle volume fraction, ρ_f is the reference density of the fluid fraction, ρ_s is the reference density of the solid fraction.
Values of $f''(0)$ for $\varphi = 0$ with $m = 2$ and $s = 0$ (impermeable surface) evaluated as Table 4[3].

Table 4 Values of f''(0) for ϕ=0 with m=2 and s=0 (impermeable surface)

λ	f''(0)
1	0
0.5	0.78032
0.2	1.13374
0.1	1.22911
0	1.311938
-0.25	1.45664
-0.5	1.49001
-0.75	1.35284
-0.95	0.94690
-0.9945	0.64502
-0.99945	0.500204
-1	0.319476

We obtained this table(Values of $f''(0)$ for $\varphi = 0$ with $m = 2$ and $s = 0$) according to Table 5.

Table 5 values of f "(0) for φ=0 with m=2 & s=0

λ	f "(0)
0.5	0.8
0.2	1.15
0.1	1.25
0	1.32
-0.25	1.46
-0.5	1.5
-0.75	1.38
-0.95	1.12

Values of $f''(0)$ for Cu nanoparticles with $m = 2$ and $s = 0.5$ in this paper[3] are given in table 5.

Table 6 Values of f''(0) for *Cu* nanoparticles with m=2 and s=0.5

	f''(0)		
λ	φ=0	φ=0.1	φ=0.2
1	0	0	0
0.5	1.1031	1.3690	1.4386
0.2	1.6614	2.0716	2.1792
0.1	1.8279	2.2835	2.4031
0	1.9839	2.4833	2.6146
-0.25	2.3229	2.9255	3.0846
-0.5	2.5785	3.2747	3.4593
-0.75	2.7298	3.5102	3.7182
-1	2.7373	3.5954	3.8255
-1.2	2.6361	3.5042	3.7535
	(0.4403)	(0.44002)	(0.44000)
-1.25	1.08223	3.4483	3.7036
	(0.5672)	(0.5634)	(0.5631)
-1.3	2.3858	3.3736	3.6360
	(0.7150)	(0.6974)	(0.6955)

That we calculate values of $f''(0)$ for this case(cu-water nanofluid , m=2 & s=0.5) as Table 6.

Table 7 Values of f "(0) for cu-water with m=2 & s=0.5

	f "(0)		
λ	φ=0	φ=0.1	φ=0.2
1	0.02	0.02	0.02
0.5	1.1	1.38	1.44
0.2	1.66	2.08	2.2
0.1	1.82	2.28	2.4
0	1.98	2.48	2.62
-0.25	2.32	2.92	3.08
-0.5	2.58	3.28	3.44
-0.75	2.74	3.5	3.72
-1	2.72	3.58	3.84
-1.2	2.58,0.36	3.5,0.4	3.76,0.42

They draw velocity profiles $f(\eta)$ for Cu nanoparticles when $m = 2$, $\varphi = 0.1$, $\lambda = -1.5$ and various values of *s as figure 8.*
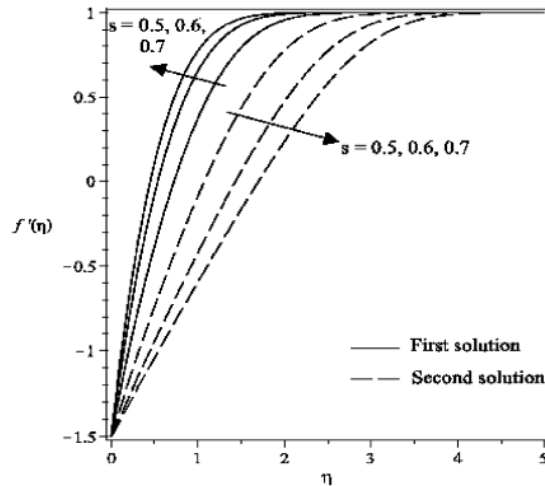
Fig.8 Velocity profiles for Cu nanoparticles when m=2, Φ=0.1, λ=-1 .5& various values of s

We obtain one of these velocity profile (for s=0.5) as Figure 9. In this figure as expected, the velocity profile approach to number 1.
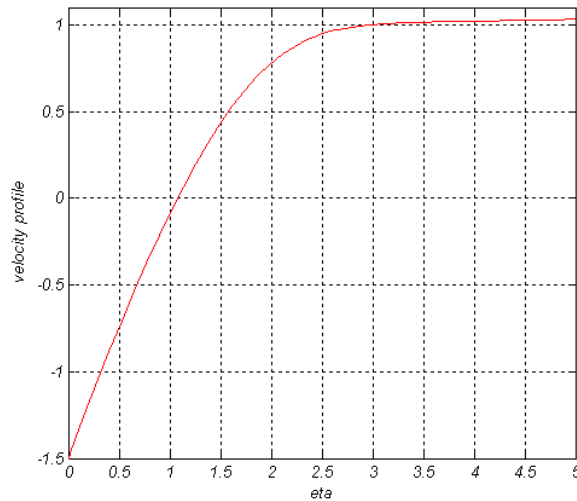

Fig.9 Velocity profile for s=0.5

Norfifah Bachok · Anuar Ishak · Ioan Pop[4] studied Boundary layer flow over a moving surface in a nanofluid with suction or injection.

The governing equation is:

$$\frac{1}{(1-\phi)^{2.5}\left(1-\phi+\frac{\phi\rho_s}{\rho_f}\right)}f''' + ff'' = 0 \tag{16}$$

With the boundary conditions as:

f(0)=f$_0$,f'(0)=λ, f'($\eta \to \infty$)=1 (17)

Variation of *f*'0) with λ for Cu-water nanofluid and different values of f_0 when φ= 0.1 in this paper [4] is given in figure 10.
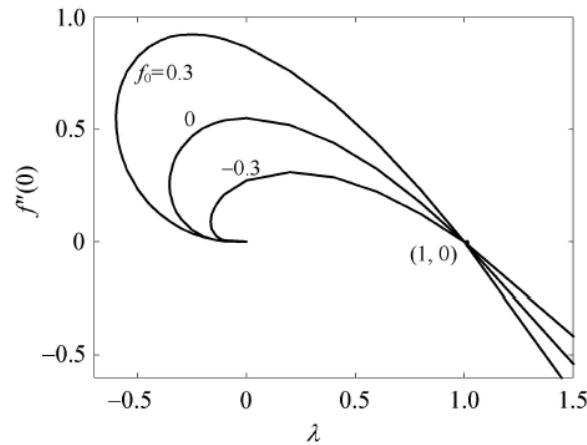
Fig.10 Variaton of f''(0) with λ for Cu-water nanofluid and different values of f_0 when $\varphi=0.1$

We obtained this variation as Table7. In this table, variaton of f''(0) with λ for Cu-water nanofluid and different values of f_0 when $\varphi=0.1$ are given.

Table 8 Values of f "(0) for cu-water when $\varphi = 0.1$

λ	f ''(0)		
	$f_0=-0.3$	$f_0=0$	$f_0=0.3$
-0.5			0.25
0	0.3	0.55	0.87
0.5	0.27	0.4	0.52
1	0.02	0.02	0.02
1.5	-0.42	-0.52	-0.67

Variation of of $f''0$) with λ for different nanoparticles when $f_0 = -0.3$ and $\varphi = 0.1$ in this paper are plotted in figure 11.
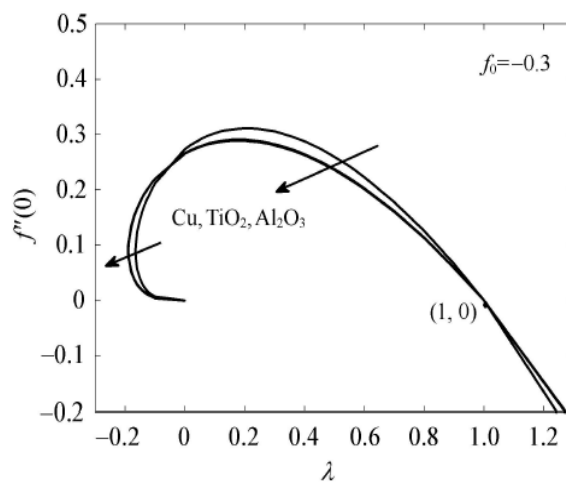

Fig.11 Variation of f''(0) with λ for defferent nanoparticles when $f_0 =-0.3$ & $\varphi= 0.1$

We obtained variation of f''(0) with λ as table 8.

Table 9 Values of f "(0) when $\varphi = 0.1$ & $f_0=-0.3$

28

λ	f''(0)
-0.2	0.1
0	0.27
0.2	0.3
0.4	0.27
0.6	0.2
0.8	0.12
1	0.02
1.2	-0.12

Velocity profiles for Cu-water nanofluid and different values of f_0 when $\lambda = -0.1$ in this paper[4] is as Figure 12:
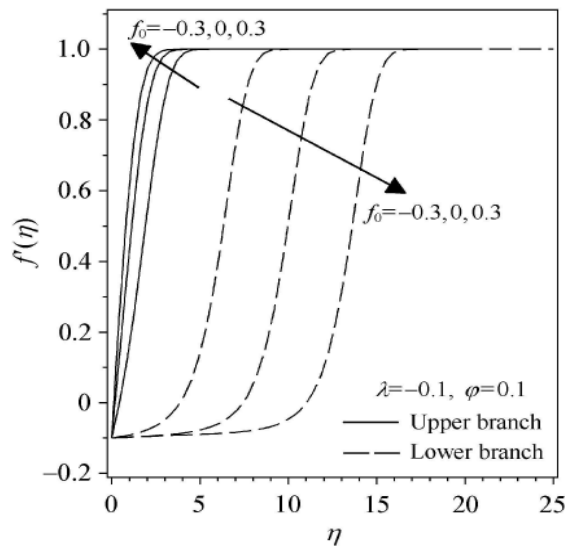

Fig.12 Velocity profiles for Cu nanoparticles and different values of f0 when λ=-0.1

We draw these profiles with Matlab software according to figure 13. As expected, all of velocity profiles are approached to 1.
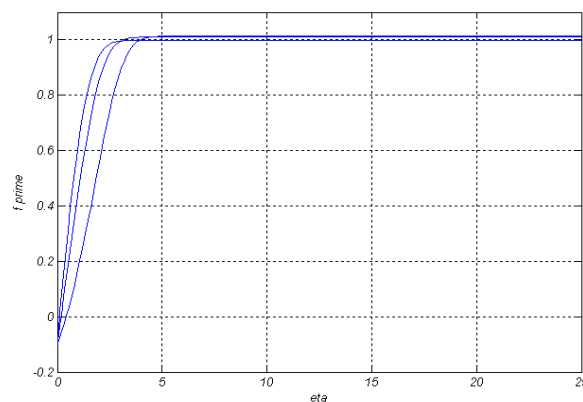

Fig.13 profiles of Cu-water nanofluid and different values of f_0

Variation of $f''0)$ with λ for different nanoparticles when $f_0 = 0.3$ and $\varphi = 0.1$ in this paper is as Figure 14.
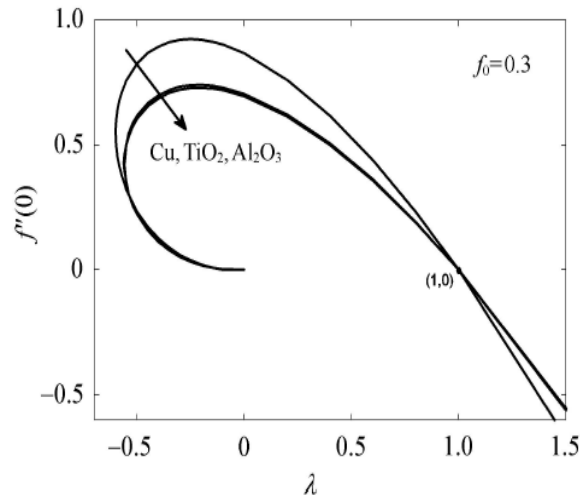
Fig.14 Variation of f''(0) with λ for different nanoparticles when $f_0 = 0.3$ and $\varphi = 0.1$

We obtained this chart with Matlab software for AL_2O_3 nanofluid as table 9.

Table 10 Values of f "(0) when $\varphi = 0.1$ & $f_0=0.3$

λ	f "(0)
-0.5	0.22
0	0.7
0.5	0.42
1	0.02
1.5	-0.55

Nor Azizah Yacob, Anuar Ishak, Ioan Pop and Kuppalapalle Vajravelu[5] survey Boundary layer flow past a stretching/shrinking surface beneath an external uniform shear flow with a convective surface boundary condition in a nanofluid.

The governing equation is:

$$(18) \quad \frac{3}{(1-\phi)^{2.5}\left(1-\phi+\frac{\phi\rho_s}{\rho_f}\right)} f''' + 2ff'' - f'^2 = 0$$

With the boundary conditions as:

f(0)=0,f'(0)=λ, f'($\eta \rightarrow \infty$)=η (19)

Variation of the skin friction coefficient namely f'0) with λ for different values of φ for Ag-water nanofluid in this paper are plotted in figure 15. It can be seen that for a particular value of λ, the skin friction coefficient increase with increasing φ.
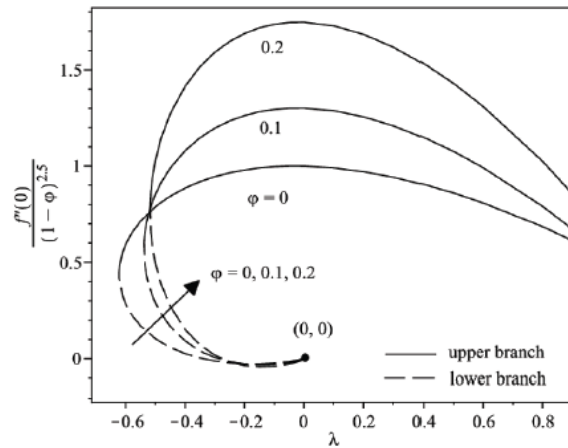
Fig.15 Variation of $f''(0)$ with λ for different values of φ for Ag-water nanofluid

We obtained this quantities as table 10.

Table 11 Variation of f "(0) with φ

	f "(0)		
λ	$\varphi=0$	$\varphi=0.1$	$\varphi=0.2$
-0.2	1	0.55	1
0	1	1	1
0.2	0.95	0.95	0.95
0.4	0.9	0.85	0.85
0.6	0.8	0.75	0.7
0.8	0.65	0.55	0.55

Variation of the skin friction coefficient namely $f''0)$ with λ when $\varphi= 0.1$ for different nanofluids and water in this paper is plotted as figure16. In general, for a particular value of λ, the skin friction coefficient of Cu-water nanofluid is higher than that of Ag-water nanofluid and that of water for the upper branch solutions, while the skin friction coefficient of Ag-water nanofluid is higher than that of Cuwater nanofluid and that of water for the lower branch solutions.
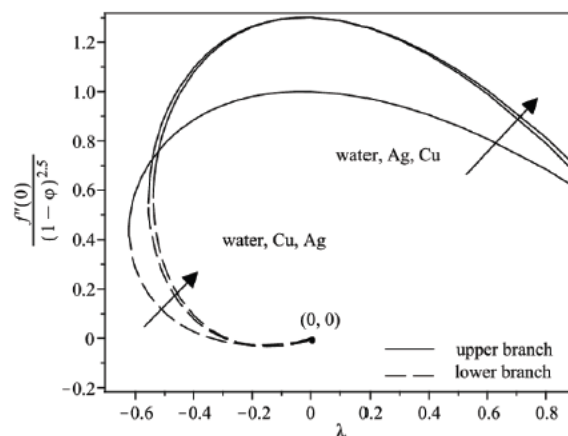

Fig.16 Variation of $f''0)$ with λ when $\varphi = 0.1$ for different nanofluids and water

We obtained this quantities with Matlab software as table 11. $\Phi=0$ is for water(pure water) and $\Phi=0.1$ is for Ag and Cu(nano fluid).

Table 12 variation of f "(0) with φ

λ	$\varphi=0$	$\varphi=0.1$
-0.4	0.95	0.9
-0.2	1	1
0	1	1
0.2	0.95	0.95
0.4	0.9	0.9
0.6	0.8	0.75
0.8	0.65	0.6

Meraj Mustafa, Muhammad A. Farooq, Tasawar Haya, Ahmed Alsaedi[6] survey Numerical and Series Solutions for Stagnation-Point Flow of Nanofluid over an Exponentially Stretching Sheet.

The governing equation is:

$$f''' + ff'' - 2f'^2 + 2\lambda^2 = 0$$
(20)

With the boundary conditions as:

$$f(0)=0, f'(0)=1, f'(\infty) \rightarrow \lambda \tag{21}$$

Numerical values of skin friction coefficient $f'(0)$ for different values of velocity ratio parameter λ in this paper is as table 12. In Table 12 $f''(0)$ on the sheet is approximated for various values of λ.

Table 13 Numerical values of skin friction coefficient $f'(0)$ for different values of velocity ratio parameter λ.

λ	
f''(0)	
0	-
1.2818	
0.1	-
1.2535	
0.2	-
1.1951	
0.5	-
0.8798	
0.8	-0.3977
1.2	0.4515

We obtained this table with as table 13. We observed that skin friction coefficient namely f''(0) is reduced by assuming sufficiently large values of λ.

Table 14 Variation of f "(0) with λ

λ	f'(0)
0	-1.3
0.1	-1.25
0.2	-1.2
0.5	-0.9
0.8	-0.4
1.2	0.45

Muatazz Abdolhadi Bashir, Mustafa Mamat and 1Ilyani Abdullah[7] survey Velocity Slip Effect on Falkner-Skan Boundary Layer Flow over a Static Wedge.

The governing equation is:

$$f''' + ff'' + \frac{2m}{m+1}(1 - f'^2) = 0 \tag{22}$$

With the boundary conditions as:

$$f(0)=0, f'(0)=Nf''(0), f'(\infty)=1 \tag{23}$$

where N is the constant velocity slip parameter.

Values of *f*'0) for various values of m when N=0 in this paper are given according to table 14.

Table 15 Values of f''(0) for various values of m when N=0

m	f''(0)
0	0.4696
1/11	0.6549
0.2	0.8021
1/3	0.9276
0.5	1.0389
1	1.2325

We obtain this table with Matlab software as table 15. The comparison of f''(0) when N=0 and the different values of m together with that were published by Muatazz Abdolhadi Bashir [7], show that our results are in good precision.

Table 16 Variation of f "(0) *with m*

m	β	f"(0)
0	0	0.6
1/11	0.16	0.65
0.2	0.33	0.8
1/3	0.5	0.95
0.5	0.66	1.05
1	1	1.25

Values of velocity profiles f', shear stress coefficient f'' for different values m & N in this paper is as table 16. Table 16 shows that the wall velocity increases with an increase in N and m.

Table 17 Values of velocity profiles, shear stress coefficient for different values m & N

m	N	f'(0)	f''(0)
0.2	0.1	0.0767	0.7674
	0.4	0.2642	0.6605
	0.7	0.3973	0.5676
	1	0.4929	0.4929
0.5	0.1	0.0972	0.9720
	0.4	0.3164	0.7910
	0.7	0.4577	0.6539
	1	0.5531	0.5531
0.8	0.1	0.1083	1.0836
	0.4	0.3429	0.8572
	0.7	0.4870	0.6958
	1	0.5814	0.5814
1.5	0.1	0.1218	1.2187
	0.4	0.3733	0.9333
	0.7	0.5196	0.7422
	1	0.6123	0.6123

That our resultes are given according to table 17. Table 17 shows that the wall share stress increases with m while it decreases with N.

Table 18 Variation of f "(0) *with m & N*

m	β	N	f"(0)
0.2	0.33	0.1	0.75
		0.4	0.65
		0.7	0.55
		1	0.5
		0.1	0.97

0.5	0.66	0.4	0.79
		0.7	0.66
		1	0.55
		0.1	1.08
0.8	0.88	0.4	0.86
		0.7	0.7
		1	0.59
		0.1	1.22
1.5	1.2	0.4	0.93
		0.7	0.75
		1	0.61

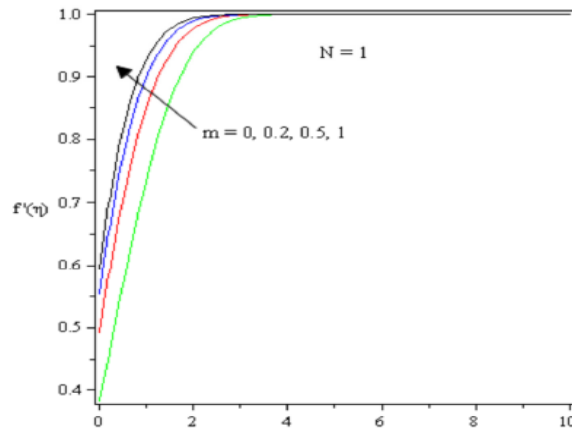Effect of m on the velocity profiles when N= 1 in this paper[7] is according to figure 17.

Fig.17 Effect of m on the velocity profiles when N= 1

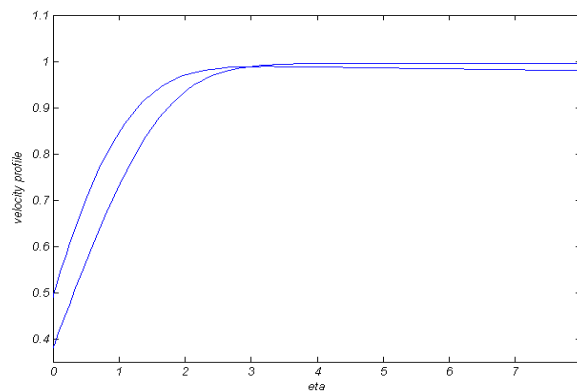We obtain this profiles with Matlab software as figure 18.

Fig.18 Effect of m on the velocity profiles when N= 1

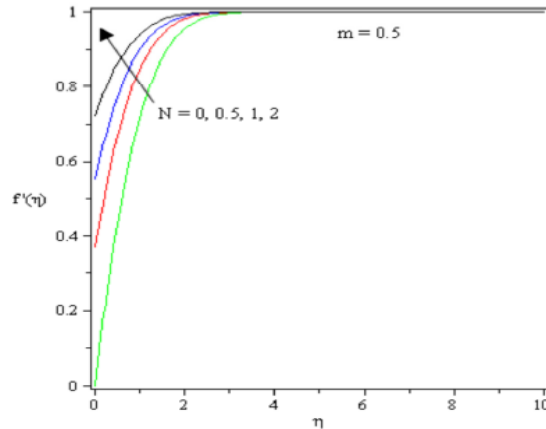Effect of N(N≥0) on the velocity, when m=0.5 in this paper is as figure 19.

Fig.19 Effect of N(N≥0) on the velocity, when m=0.5

We obtain this profiles as figure 20. This figure shows that the velocity increases with the increase of the slip parameter(N).
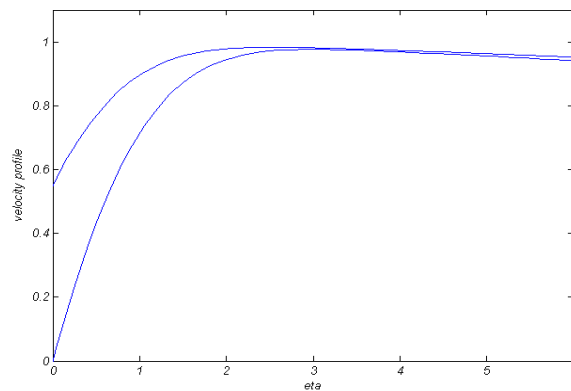

Fig.20 Effect of N(N≥0) on the velocity, when m=0.5

IV. CONCLUSION

Flow over a wedge was analyzed incorporating a slip and nonslip boundary condition. This problem was solved for Newtonian fluid and compared with nanofluid. Also the problem of forced convection boundary layer flow near the stagnation point on a permeable stretching/shrinking surface in a nanofluid is studied theoretically. We solved these ODE equations with Matlab software and compared our results with the published corresponding papers. These comparisons showed that our results are with good precision and are according to published papers.

REFERENCES

[1]   Choi, S.U.S. Enhancing thermal conductivity of fluids with nanoparticles. Siginer, D.A., Wang, H.P. eds. Developments and Applications of Non-Newtonian Flows. FEDvol. 231 66, 99–105 (1995)

[2]   B.D. Ganapol. Highly Accurate Solutions of the Blasius and Falkner-Skan Boundary Layer Equations via Convergence Acceleration.
        Department of Aerospace and Mechanical Engineering University of Arizona.

[3]   Norihan MD. Arifin, Roslinda Nazar & Ioan Pop. Viscous flow due to a permeable stretching/shrinking sheet in a nanofluid.(2011)

[4]   Norfifah Bachok, Anuar Ishak & Ioan Pop. Boundary layer flow over a moving surface in a nanofluid with suction or injection. The chinese society of theoretical and applied mechanics and springer-verlag berlin heidelberg.(2012)

[5]   Nor Azizah Yacob, Anuar Ishak, Ioan Pop & Kuppalapalle Vajravelu. Boundary layer flow past a stretching/shrinking surface beneath an external uniform shear flow with a convective surface boundary condition in a nanofluid. nanoscale research letters. (2011)

[6]   Meraj Mustafa, Muhammad A. Farooq, Tasawar Haya, Ahmed Alsaedi. Numerical and series solutions for stagnation-point flow of nanofluid over an exponentially stretching sheet.

[7]   Muatazz Abdolhadi Bashir, Mustafa Mamat and 1ilyani Abdullah. Velocity slip effect on falkner-skan boundary layer flow over a static wedge. adv. studies theor. phys., vol. 7, 2013, no. 6, 277 - 286.

[8]   Yina sun, Xinhai Si and Yanan Shen. DTM-BF method for the flow and heat transfer of a nanofluid over a stretching or shrinking sheet. international journal on numerical methods in engineering vol.1, n.2, april 2013

[9]   A. P. M.Fallah, A. Moradi, T. Hayat, Awatif A. Hendi. Pareto optimization of nanofluid falkner-skan wedge flow using genetic algorithm based on neural network modeling. iam, v.1, n.1, 2012, pp.15-35

[10]   Waqar A. Khan and I. Pop. Boundary layer flow past a wedge moving in a nanofluid. Hindawi publishing corporation mathematical problems in engineering volume 2013.

[11]   Kourosh Parand, Nasrollah Pakniat, Zahra Delafkar. Numerical solution of the falkner-skan equation with stretching boundary by collocation method. international journal of nonlinear science vol.11(2011) no.3,pp.275-283.

[12]   Michael J. Martin and Iain D. Boyd. Falkner–Skan flow over a wedge with slip boundary conditions. journal of thermophysics and heat transfer vol. 24, no. 2, april–june 2010.

[13]   Fathi M Allan and Mohamed a Hajji. On the similarity solution of nano-fluid flow over a moving flat plate using the homotopy analysis method.

[14]   Miccal T. Matthews, James M. Hill. A note on the boundary layer equations with linear slip boundary condition. Applied mathematics letters 21 (2008) 810–813.

[15]   Norfifah Bachok & Anuar Ishak. Similarity solutions for the stagnation-point flow and heat transfer over a nonlinearly stretching/shrinking sheet. sains malaysiana 40(11)(2011): 1297–1300

[16]   Eleanor D. Kaufman. Velocities, pressures and temperature distributions near a stagnation point in planar incompressible flow. may 2008.

[17]   Okedayo T. Gideon, Olanrewaju P. O. , Gbadeyan J. A. Analysis of convective plane stagnation point flow with convective boundary conditions. international journal of science and technology. volume 2 no.1, january 2012.

[18]   C. Y. Wang and Chiu-on NG. Stagnation flow on a heated vertical plate with surface slip. Journal of heat transfer. july 2013, vol. 135 / 074505-1

[19]   Vai Kuong Sin and Tai Yin Tong. Stagnation-point pressure distribution and wall shear stress: numerical simulation and similarity solution. World congress on engineering 2009 vol ii.

[20]   *F. Mohammadi, M.M. Hosseini, A. Dehgahn and F.M. Maalek Ghaini.* Numerical solutions of falkner-skan equation with heat transfer. studies in nonlinear sciences 3 (3): 86-93, 2012.

[21]   H. Bararnia, N. Haghparast, MO. Miansari and A. Barari. Flow analysis for the falkner–skan wedge flow.

[22]   Michael J. Martin and Iain D. Boyd. Falkner–Skan flow over a wedge with slip boundary conditions. Journal of thermophysics and heat transfer vol. 24, no. 2, april–june 2010.

[23]   J. Singh. Asymptotic behaviour of the solutions of the falkner-skan equations governing the swirling flow. adv. theor. appl. mech., vol. 3, 2010, no. 4, 151 – 158.

[24]   L. Quartapelle and A. Scandroglio. Solution of the falkner–skan equation to determine reverse flow. 18 may 2006.

[25]   Jiawei Zhang Binghe Chen. An iterative method for solving the Falkner-Skan equation.